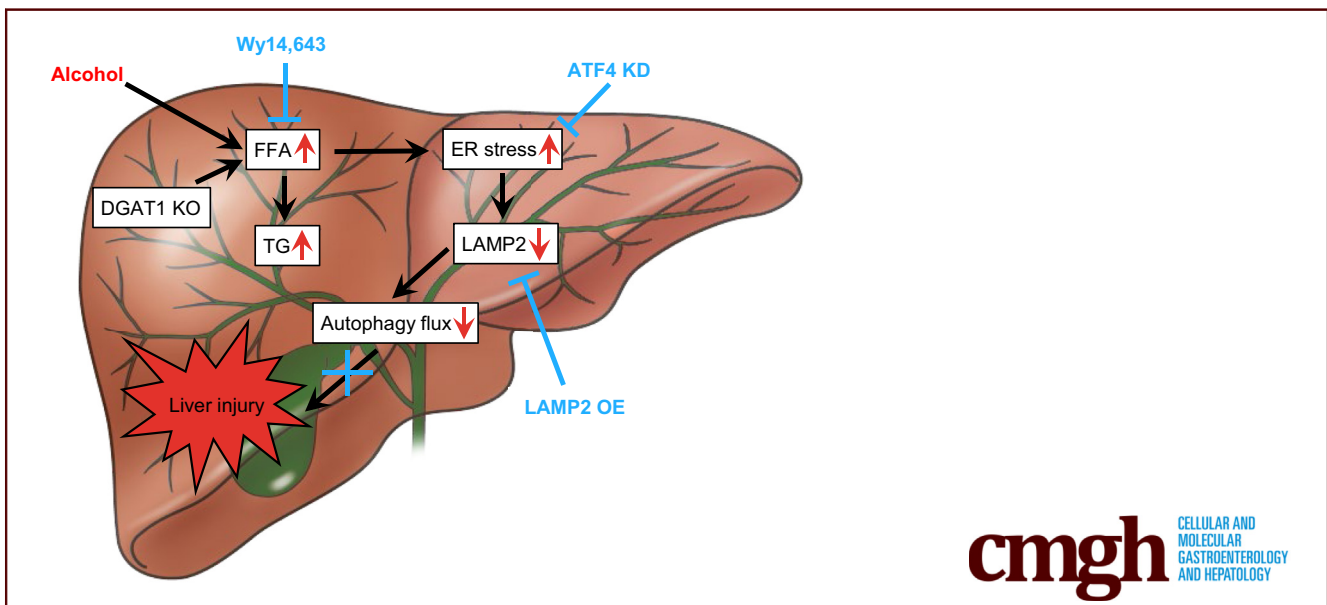


## ORIGINAL RESEARCH

## Fatty Acids Inhibit LAMP2-Mediated Autophagy Flux via Activating ER Stress Pathway in Alcohol-Related Liver Disease

Wei Guo,<sup>1</sup> Wei Zhong,<sup>1,2</sup> Liuyi Hao,<sup>1</sup> Haibo Dong,<sup>1</sup> Xinguo Sun,<sup>1</sup> Ruichao Yue,<sup>1</sup> Tianjiao Li,<sup>2</sup> and Zhanxiang Zhou<sup>1,2</sup><sup>1</sup>Center for Translational Biomedical Research and <sup>2</sup>Department of Nutrition, University of North Carolina at Greensboro, North Carolina Research Campus, Kannapolis, North Carolina

## SUMMARY

Accumulation of hepatic free fatty acids (FFAs) induces hepatocellular ER stress, which, in turn, represses LAMP2 expression and thereby impairs autophagy flux in alcohol-related liver disease (ALD). Reducing hepatic FFA levels ameliorates ER stress-impaired LAMP2-autophagy flux, leading to reversal of ALD.

**BACKGROUND & AIMS:** Alcohol-related liver disease (ALD) is characterized by accumulation of hepatic free fatty acids (FFAs) and triglyceride (TG)-enriched lipid droplets and cell death. The present study aimed to investigate how FFA or TG induces hepatocyte injury, thereby contributing to the development of ALD.

**METHODS:** Hepatocyte-specific DGAT1 knockout (DGAT1<sup>Δhep</sup>) mice and lysosome-associated membrane protein 2 (LAMP2) overexpression mice were generated and subjected to chronic alcohol feeding. Cell studies were conducted to define the causal role and underlying mechanism of FFA-induced hepatocellular injury.

**RESULTS:** Hepatocyte-specific DGAT1 deletion exacerbated alcohol-induced liver injury by increasing lipid accumulation and endoplasmic reticulum (ER) stress, reducing LAMP2 protein levels, and impairing autophagy function. Cell studies revealed that FFAs, rather than TG, induced ER stress via ATF4 activation, which, in turn, down-regulated LAMP2, thereby impairing autophagy flux. LAMP2 overexpression in the liver restored autophagy function and ameliorated alcohol-induced liver injury in mice. Reducing hepatic FFAs by peroxisome proliferator-activated receptor  $\alpha$  activation attenuated ER stress, restored LAMP2 protein levels, and improved autophagy flux. In addition, suppression of LAMP2 and autophagy function was also detected in the liver of patients with severe alcoholic hepatitis.

**CONCLUSIONS:** This study demonstrates that accumulation of hepatic FFAs, rather than TG, plays a crucial role in the pathogenesis of ALD by suppressing LAMP2-autophagy flux pathway through ER stress signaling, which represents an important mechanism of FFA-induced hepatocellular injury in ALD. (*Cell Mol Gastroenterol Hepatol* 2021;12:1599–1615; <https://doi.org/10.1016/j.jcmgh.2021.07.002>)

**Keywords:** Free Fatty Acid; DGAT1; Lipotoxicity; Autophagy; Alcohol-Induced Liver Injury.

Excessive alcohol consumption is widely recognized as a major social and health problem all over the world. In the United States, alcohol use disorder is the third leading cause of preventable death, and the estimated annual cost for alcohol use disorder is nearly \$250 billion.<sup>1,2</sup> Among the many medical diseases associated with alcohol consumption, alcohol-related liver disease (ALD) contributes to the majority of mortality.<sup>3</sup> This disease encompasses a wide spectrum of clinical conditions, including alcoholic steatosis, hepatitis, and fibrosis, which may progress to cirrhosis and even hepatocellular carcinoma.<sup>4</sup> Despite great efforts that have been made in understanding the molecular mechanisms, there are currently no effective therapies available for the treatment of ALD.

Liver is the central organ that regulates fatty acid metabolism. Under physiological conditions, excessive fatty acids in the liver are converted into triglycerides (TGs), which are exported to blood via very-low-density lipoprotein (VLDL) secretion and stored in white adipose tissue. During fasting, TG stored in adipose tissue is hydrolyzed to free fatty acids (FFAs) for use by other tissues including the liver. Our lab and others have demonstrated that chronic alcohol consumption increases adipose tissue lipolysis, leading to excessive release of FFAs into the bloodstream and subsequent increase of hepatic FFAs import and accumulation.<sup>5,6</sup> In addition, alcohol intake has been shown to reduce hepatic fatty acid oxidation, which also contributes to the accumulation of FFAs in the liver.<sup>7,8</sup> Although it is generally accepted that prolonged hepatic lipid accumulation can progress to more severe stages of liver diseases, growing evidence also suggests that FFAs and their metabolites, compared with TG, generate more lipotoxicity and subsequent damages to organelles such as mitochondria, peroxisome, and endoplasmic reticulum (ER).<sup>9–12</sup>

Autophagy is an evolutionarily conserved catabolic process involved in the breakdown and removal of cytosolic organelles, lipids, and proteins by lysosome, which is essential for maintaining cellular homeostasis.<sup>13,14</sup> A number of studies have revealed that autophagy plays an important role in the pathogenesis of numerous diseases including ALD.<sup>15,16</sup> Accumulating evidence has demonstrated that chronic alcohol exposure leads to hepatic lysosome dysfunction and protein accumulation.<sup>17,18</sup> Although recent investigations have shown that autophagy contributes to hepatic lipid metabolism,<sup>16,19–22</sup> the effects and mechanisms of FFAs on autophagy have not been fully understood.

In mammalian cells, FFAs are incorporated into TG by two acyl-CoA:diacylglycerol acyltransferases (DGATs), namely DGAT1 and DGAT2, that belong to distinct acyltransferase families.<sup>23</sup> Both enzymes are abundantly expressed in tissues associated with TG metabolism, such as adipose tissue, liver, and small intestine.<sup>24</sup> In the liver, it has been reported that DGAT2 preferentially uses fatty acids from de novo lipogenesis for TG synthesis.<sup>25</sup> In contrast, DGAT1 mainly uses exogenous fatty acids for TG synthesis because mice lacking hepatic DGAT1 are only protected from high-fat-diet-induced hepatic steatosis, but

not from steatosis induced by up-regulated de novo lipogenesis.<sup>26</sup>


A growing number of studies have demonstrated that neutral TG-enriched lipid droplets synthesis and accumulation, which may serve as a detoxification process, protect liver against FFA-induced cytotoxicity and organelle damage, therefore promoting cell viability.<sup>27–29</sup> Earlier reports revealed that chronic alcohol intake leads to autophagy dysfunction such as impaired autophagy flux.<sup>30,31</sup> Considering that alcohol consumption increases fatty acid flux from blood to the liver and DGAT1 is primarily responsible for synthesizing TG from exogenous FFAs, we aimed to determine whether hepatocyte-specific DGAT1 deletion affects hepatic lipid homeostasis and autophagy function, thereby modulating the progression of ALD. For this purpose, we generated hepatocyte-specific DGAT1 knockout (DGAT1<sup>Δhep</sup>) mice and fed them with Lieber-DeCarli ethanol liquid diets. We further performed in vitro cell culture studies, in vivo LAMP2 overexpression, and reversal experiment that reduced FFA accumulation to explore how hepatic FFAs elicit the deleterious effects in the liver during the pathogenesis of ALD. Our results provide insights into an inhibitory effect of FFAs on autophagy flux in the progression of ALD as well as the underlying mechanisms.

## Results

### *DGAT1 Deletion in Hepatocytes Worsens Alcohol-Induced Hepatic Lipid Accumulation via Impairing VLDL Lipidation in Mice*

We first confirmed that chronic alcohol feeding increased DGAT1 levels in mouse liver (Figure 1A). At the same time, hepatic DGAT2 was also up-regulated by alcohol feeding (Figure 1A). We then generated hepatocyte-specific DGAT1 knockout mice (DGAT1<sup>Δhep</sup>) to investigate how DGAT1 deletion in hepatocytes may affect the pathogenesis of ALD. To validate the knockout efficiency, we performed quantitative polymerase chain reaction analysis and confirmed that DGAT1 was successfully deleted in mouse liver (Figure 1B). There was a slight increase in the mRNA levels of hepatic DGAT2 along with DGAT1 deletion (Figure 1B). Floxed mice and DGAT1<sup>Δhep</sup> mice were then subjected to chronic feeding with control (pair-fed [PF]) or alcohol (alcohol-fed [AF]) liquid diet. Hepatic FFA levels

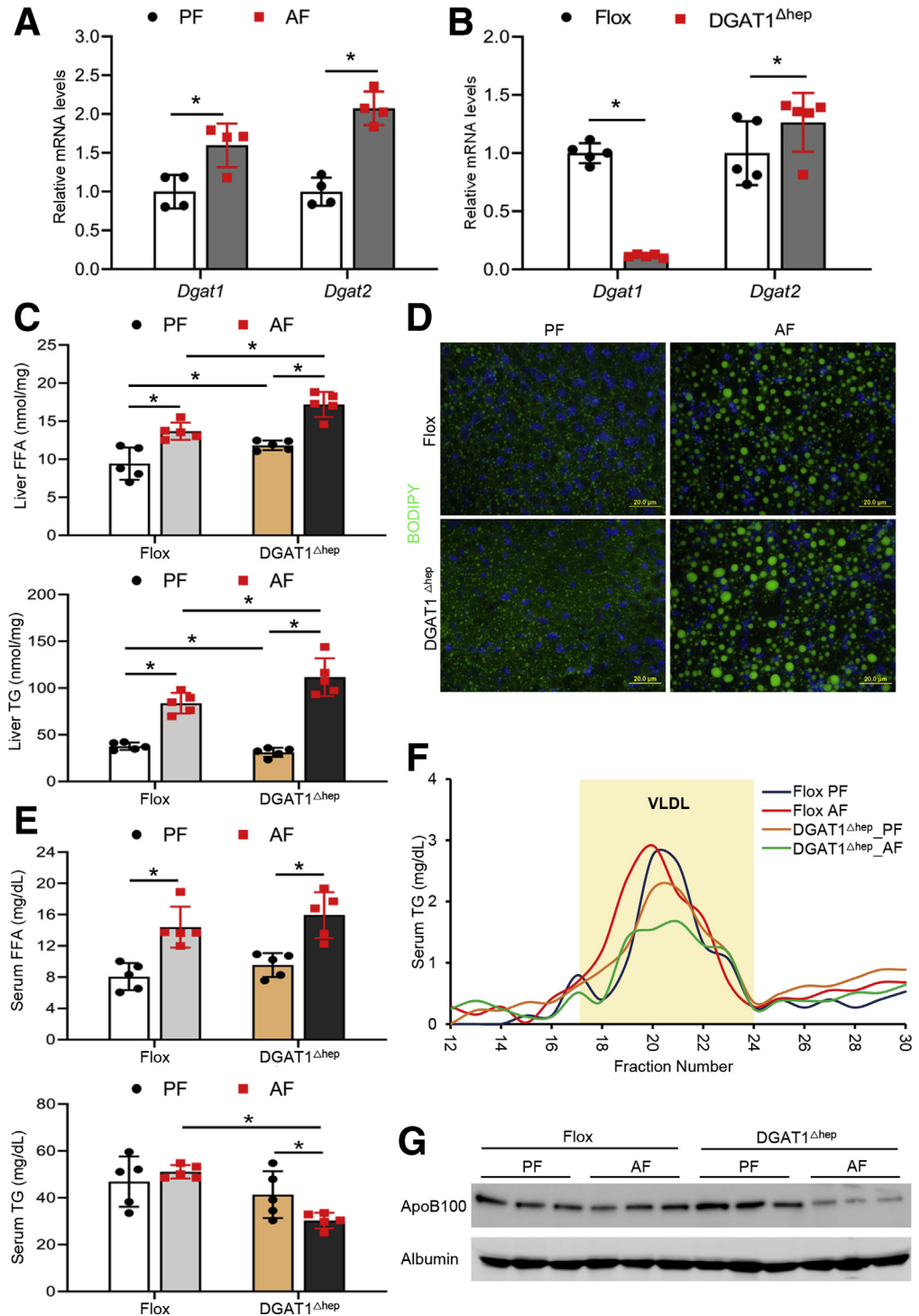
**Abbreviations used in this paper:** AF, alcohol-fed; ALD, alcohol-related liver disease; ALT, alanine aminotransferase; AST, aspartate aminotransferase; ATF4, activating transcription factor 4; CHOP, C/EBP homologous protein; DGAT1, acyl-CoA:diacylglycerol acyltransferase 1; ER, endoplasmic reticulum; FFA, free fatty acid; LAMP2, lysosome-associated membrane protein 2; LC3II, microtubule-associated protein 1A/1B-light chain 3 II; LDH, lactate dehydrogenase; MPO, myeloperoxidase; OA, oleic acid; PA, palmitic acid; PF, pair-fed; PPAR $\alpha$ , peroxisome proliferator-activated receptor  $\alpha$ ; SAH, severe alcoholic hepatitis; TG, triglyceride; VLDL, very-low-density lipoprotein.

 Most current article

© 2021 The Authors. Published by Elsevier Inc. on behalf of the AGA Institute. This is an open access article under the CC BY-NC-ND license (<http://creativecommons.org/licenses/by-nc-nd/4.0/>).

2352-345X

<https://doi.org/10.1016/j.jcmgh.2021.07.002>



were elevated in PF DGAT1<sup>Δhep</sup> mice compared with PF floxed mice, whereas a further increase was found in AF DGAT1<sup>Δhep</sup> mice (Figure 1C). Unexpectedly, DGAT1 deletion exacerbated alcohol-induced hepatic TG accumulation (Figure 1C). Alcohol feeding induced neutral lipid droplets accumulation in the liver of AF floxed mice, which was further increased in AF DGAT1<sup>Δhep</sup> mice (Figure 1D). Alcohol feeding increased serum FFA levels, and DGAT1 ablation had no additional impact (Figure 1E). Although

serum TG levels were not affected by either alcohol feeding or DGAT1 deletion, they were markedly suppressed in AF DGAT1<sup>Δhep</sup> mice (Figure 1E). A previous study has reported that DGAT1 is essential for lipidation and maturation of hepatic VLDL particles, which are then secreted into the blood.<sup>32</sup> Thus, we evaluated whether DGAT1 knockout would affect serum VLDL levels. Fast protein liquid chromatography analysis demonstrated that the TG concentration in serum VLDL (fractions 17~24) was decreased in PF

DGAT1<sup>Δhep</sup> mice, and a further decrease was observed in AF DGAT1<sup>Δhep</sup> mice (Figure 1F). In accordance, serum protein levels of apolipoprotein B100 were reduced by alcohol feeding, and a further reduction was observed in AF DGAT1<sup>Δhep</sup> mice (Figure 1G). Collectively, these data suggest that hepatocyte-specific DGAT1 ablation increases hepatic lipid contents possibly through impairing VLDL lipidation and secretion.

### Hepatocyte-Specific DGAT1 Deletion Exacerbates Alcohol-Induced Liver Injury in Mice

Next, we examined the effect of hepatocyte-specific DGAT1 deletion on alcohol-induced liver damage. We found that serum alanine aminotransferase (ALT) and aspartate aminotransferase (AST) levels were both significantly increased in AF DGAT1<sup>Δhep</sup> mice compared with AF floxed mice (Figure 2A). Alcohol-induced lipid droplets accumulation and hepatocyte necrotic degeneration, as indicated by enlarged cell size and nucleus disappearance, were aggravated by DGAT1 deletion (Figure 2B). Alcohol feeding induced apoptotic cell death in floxed mice as indicated by deoxyuride-5'-triphosphate biotin nick end labeling (TUNEL) positive nuclei, and AF DGAT1<sup>Δhep</sup> mice had the most positive cells (Figure 2C). Moreover, DGAT1 deletion exacerbated alcohol-induced oxidative stress in the liver, as indicated by augmented lipid peroxidation (Figure 2D). We also examined the impact of hepatocyte DGAT1 knockout on hepatic inflammation. Quantitative polymerase chain reaction analysis showed that the mRNA levels of C-X-C motif chemokine ligand 1 (*Cxcl1*), a neutrophil chemoattractant, and lymphocyte antigen 6G (*Ly6g*), a marker of neutrophil, were markedly increased in AF DGAT1<sup>Δhep</sup> mice compared with AF floxed mice (Figure 2E). Alcohol-induced hepatic neutrophil infiltration was further elevated by DGAT1 deletion as observed by increased number of myeloperoxidase (MPO) positive cells, indicating augmented inflammation in the liver (Figure 2F). These results suggest that hepatocyte-specific DGAT1 depletion exacerbates alcohol-induced liver injury.

### Alcohol-Induced Organelle Dysfunction Was Aggravated by Hepatocyte-Specific DGAT1 Deletion in Mice

Because earlier studies have reported that FFAs induce ER stress and autophagy dysfunction,<sup>21</sup> we evaluated markers of ER stress and autophagy and found that alcohol-induced hepatic activating transcription factor 4 (ATF4) and C/EBP homologous protein (CHOP) activation were aggravated in DGAT1<sup>Δhep</sup> mice (Figure 3A and B). The level of a typical lysosomal protein, lysosomal-associated membrane protein 1 (LAMP1), was not affected by either alcohol or DGAT1 deletion (Figure 3A). However, alcohol feeding resulted in the suppression of another key lysosomal protein, LAMP2, which was exaggerated by DGAT1 knockout (Figure 3A and C). Microtubule-associated protein light chain 3 II (LC3II) is a protein involved in the autophagy process, and its accumulation indicates blockade of

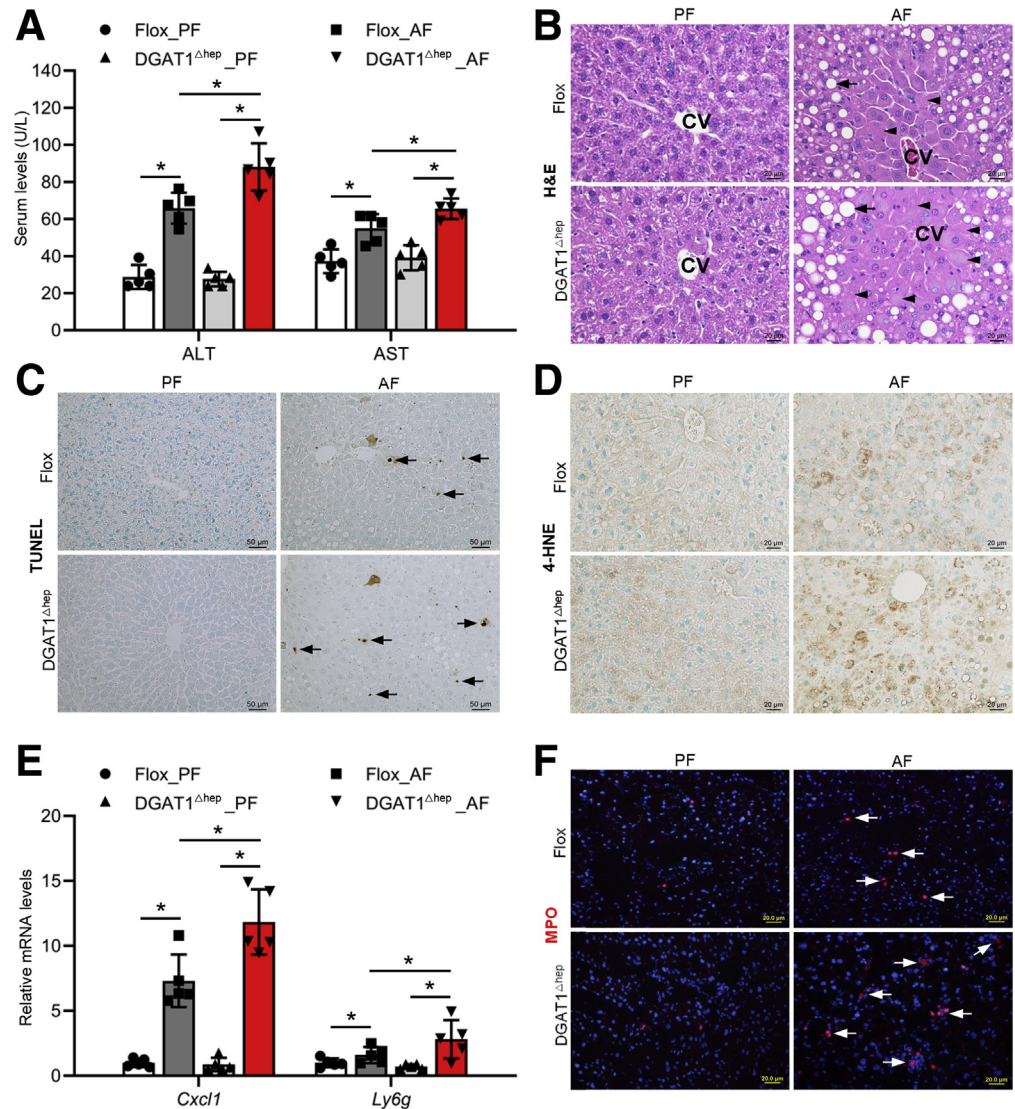
autophagy flux.<sup>33</sup> Alcohol feeding led to a marked increase of hepatic LC3II in both floxed and DGAT1<sup>Δhep</sup> mice (Figure 3A). These results suggest that hepatocyte-specific DGAT1 depletion exacerbates alcohol-induced hepatic organelle dysfunction by increasing ER stress and impairing autophagy function.

### FFAs but not TG Induce ER Stress and Autophagy Dysfunction in Hepatocytes

We next sought to dissect the role of FFAs and TG on the induction of ER stress and autophagy dysfunction because both were increased in mouse liver after DGAT1 deletion. We hypothesized that saturated FFAs induce greater hepatocellular injury and organelle dysfunction because of their limited ability to be converted into TG. Co-treatment with unsaturated FFA will attenuate such cytotoxicity by enhancing the conversion of saturated FFAs into TG, therefore improving cell viability. Hepa-1c1c7 cells were treated with palmitic acid (PA), oleic acid (OA), or a combination of PA and OA (PA+OA) for 24 hours. BODIPY staining of neutral lipids showed that cells treated with PA had the least accumulation of lipid droplets, whereas both OA and PA+OA treatments caused substantial accumulation of lipid droplets (Figure 4A). Biochemical analyses showed that PA, but not OA, increased cellular FFA levels, and OA co-supplementation attenuated PA-induced cellular FFAs accumulation (Figure 4B). Compared with PA only treatment, both OA and PA+OA treatments significantly increased cellular TG levels, with the combined treatment yielding the highest amount (Figure 4B). In accordance, PA treatment led to an elevated lactate dehydrogenase (LDH) release to the medium, an indicator of cellular injury (Figure 4C). Immunoblot analysis revealed that PA up-regulated the protein levels of ATF4, CHOP, and LC3II and reduced LAMP2, whereas LAMP1 was not affected (Figure 4D). Considering the important role of LAMP2 in autophagosome-lysosome fusion, the data of PA-mediated LAMP2 reduction and LC3II accumulation suggest that the process of autophagy flux may be impaired by FFAs. To monitor autophagy flux, Hepa-1c1c7 cells were transiently transfected with a tandem-tagged ptfLC3 (mRFP-EGFP-LC3) and treated with fatty acids. Successful fusion will lead to the virtualization of only mRFP fluorescence signal because the green fluorescent protein signals will be quenched in acidic environment inside the autolysosome. As expected, only mRFP signals were detected in OA- or PA+OA-treated cells, whereas PA treatment alone increased the amount of both GFP and mRFP signals within the cells (Figure 4E). The merged image of PA-treated cells yielded a yellow signal, indicating a blockade of autophagy flux (Figure 4E). Consistently, flow cytometry analysis confirmed that PA treatment induced more cellular injury and apoptosis (Annexin V-positive cells) (Figure 4F). Collectively, the results indicate that FFAs, rather than TG, induce hepatocellular injury via inhibition of LAMP2-mediated autophagy flux.

### Figure 2. Hepatocyte-specific DGAT1 knockout exacerbates alcohol-induced liver injury in mice.

Floxed and DGAT1<sup>Δhep</sup> mice were PF or AF for 8 weeks. (A) Analysis of serum ALT and AST levels (n = 5/group). (B) H&E staining of liver tissue sections (n = 5/group). Scale bars, 20 μm. Arrowheads: hepatocyte degeneration. Arrows: hepatic lipid droplets. CV, central vein. (C) Immunohistochemistry analysis of TUNEL on liver tissue sections (n = 5/group). Scale bars: 50 μm. Arrow: TUNEL positive cells. (D) Immunohistochemistry staining of 4-HNE on liver tissue sections (n = 5/group). Scale bars, 20 μm. (E) *Cxcl1* and *Ly6g* mRNA expression (n = 5/group). (F) Immunofluorescence staining of hepatic MPO positive cells (red) (n = 5/group). Scale bars, 20 μm. Data are shown as means ± SD. \*P < .05.



### LAMP2 Reduction Is a Direct Downstream Event of ER Stress in Hepatocytes

Because both our animal and cell studies showed a reduction of LAMP2 in association with increased ER stress, a possible link between ER stress and LAMP2 was further defined. Hepa-1c1c7 cells were treated with tunicamycin, an ER stress inducer, for 24 hours. As shown in Figure 5A, a strong activation of ATF4 and CHOP was observed on tunicamycin treatment, whereas LAMP2 protein was markedly reduced. Immunofluorescence microscopy also confirmed that tunicamycin treatment led to a strong induction of ATF4, whereas LAMP2 was barely detectable (Figure 5B). Next, we created a stable ATF4 knockdown cell line and treated the cells with PA. We found that PA-induced ATF4 and CHOP protein levels were largely abrogated by ATF4 knockdown, whereas PA-suppressed LAMP2 protein levels were restored (Figure 5C). Moreover, PA-induced LC3II accumulation was

normalized by ATF4 knockdown (Figure 5C). These data suggest that suppression of LAMP2 is a downstream event of ER stress, and suppressing ER stress improves autophagy function.

### Hepatocyte-Specific LAMP2 Overexpression Ameliorates Alcohol-Induced Organelle Dysfunction in Mice

To further determine whether LAMP2 facilitates autophagy function and thereby alleviates ER stress, hepatocyte-specific LAMP2 overexpressing (AAV8-TBG-m-LAMP2) mice were created and subjected to chronic alcohol feeding. Alcohol-suppressed LAMP2 mRNA was fully restored in LAMP2 transgenic mice to a level that was even higher than PF mice (Figure 6A). Consistently, Western blot and immunohistochemistry staining demonstrated that the decreased LAMP2 protein levels

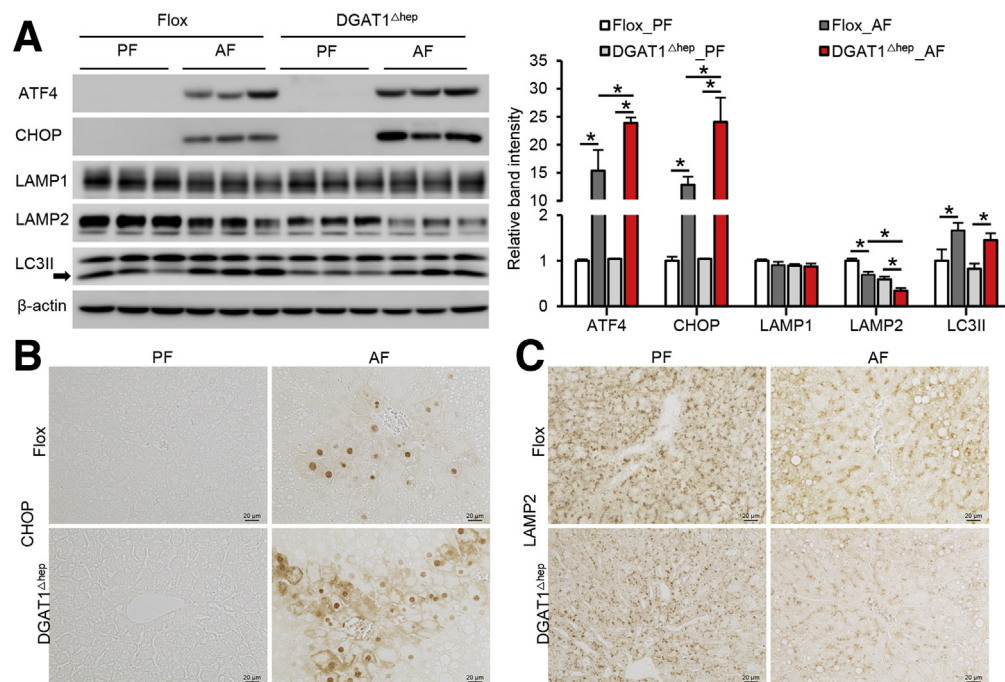


**Figure 3. Alcohol-induced organelle dysfunction was aggravated by hepatocyte-specific DGAT1 deletion in mice.** (A) Immunoblot and quantification analysis of hepatic protein levels of ATF4, CHOP, LAMP1, LAMP2, and LC3II (n = 5/group). (B and C) Immunohistochemistry analysis of CHOP (left) and LAMP2 (right) of liver tissue sections (n = 3/group). Scale bars, 20  $\mu$ m. Data are shown as means  $\pm$  SD. \* $P < .05$ .

were fully reversed in LAMP2 transgenic mice without affecting LAMP1 (Figure 6A and B). Along with LAMP2 overexpression, alcohol-elevated hepatic protein levels of LC3II were normalized in AAV8-LAMP2 mice, suggesting improvement of autophagy function (Figure 6C). Interestingly, LAMP2 overexpression also alleviated alcohol-induced hepatic ER stress as indicated by reduced protein levels of ATF4 and CHOP (Figure 6C and D).

#### Hepatocyte-Specific LAMP2 Overexpression Attenuates Alcohol-Induced Lipid Accumulation and Liver Injury in Mice

We next examined the effect of hepatocyte-specific LAMP2 overexpression on alcohol-induced liver damage. Alcohol-induced hepatic accumulation of FFAs and TG (Figure 7A) as well as BODIPY-positive neutral lipid droplets (Figure 7B) was ameliorated by LAMP2 overexpression. Hepatocellular injury was assessed by measuring serum ALT and AST as well as histopathologic changes. LAMP2 overexpression prevented alcohol-induced elevation of serum ALT and AST levels (Figure 7C) and reduced hepatocyte necrotic degeneration (Figure 7D). Alcohol-induced hepatic inflammation as indicated by up-regulated Cxcl1 and Ly6g mRNA expression and infiltrated MPO-positive neutrophils (Figure 7F) were also attenuated by LAMP2 overexpression. These data suggest that hepatocyte-specific LAMP2 overexpression protects against alcohol-induced lipid accumulation and liver injury.

#### Pharmacologic Activation of Peroxisome Proliferator-Activated Receptor $\alpha$ Accelerates Fatty Acid Metabolism and Reverses Alcohol-Induced Liver Injury

Peroxisome proliferator-activated receptor  $\alpha$  (PPAR $\alpha$ ) is a ligand-activated nuclear transcription factor, and many of its target genes are key enzymes in fatty acid metabolism.<sup>34</sup> Because DGAT1 deletion in the liver further increased alcohol-induced hepatic FFAs level and worsened alcohol-induced liver injury, we sought to determine whether using a potent PPAR $\alpha$  agonist, Wy14,643, to decrease hepatic FFA levels would reverse alcohol-induced organelle dysfunction and liver damage. We first confirmed that Wy14,643 successfully activated PPAR $\alpha$  by the induction of several PPAR $\alpha$  target proteins involved in fatty acid activation and fatty acid  $\beta$ -oxidation, including acyl-CoA synthetase long chain family member 1, acyl-CoA dehydrogenase long chain, acyl-CoA dehydrogenase medium chain, and acyl-CoA oxidase 1 (Figure 8A). Under the condition of alcohol feeding, DGAT1 deletion-induced FFAs and TG accumulation was reversed by Wy14,643 supplementation (Figure 8B). Wy14,643 also improved alcohol-induced liver injury in AF DGAT1<sup>Δhep</sup> mice as indicated by attenuation of serum ALT and AST elevation (Figure 8C), hepatocyte lipid droplet accumulation, and hepatocyte necrotic degeneration (Figure 8D). In addition, Wy14,643 supplementation alleviated ER stress in the liver of DGAT1<sup>Δhep</sup> AF mice as indicated by decreased protein levels of ATF4 and CHOP (Figure 8E and F). The suppressed LAMP2 protein was restored, and LC3II accumulation was alleviated in the liver of AF DGAT1<sup>Δhep</sup> mice with Wy14,643 (Figure 8E and G).

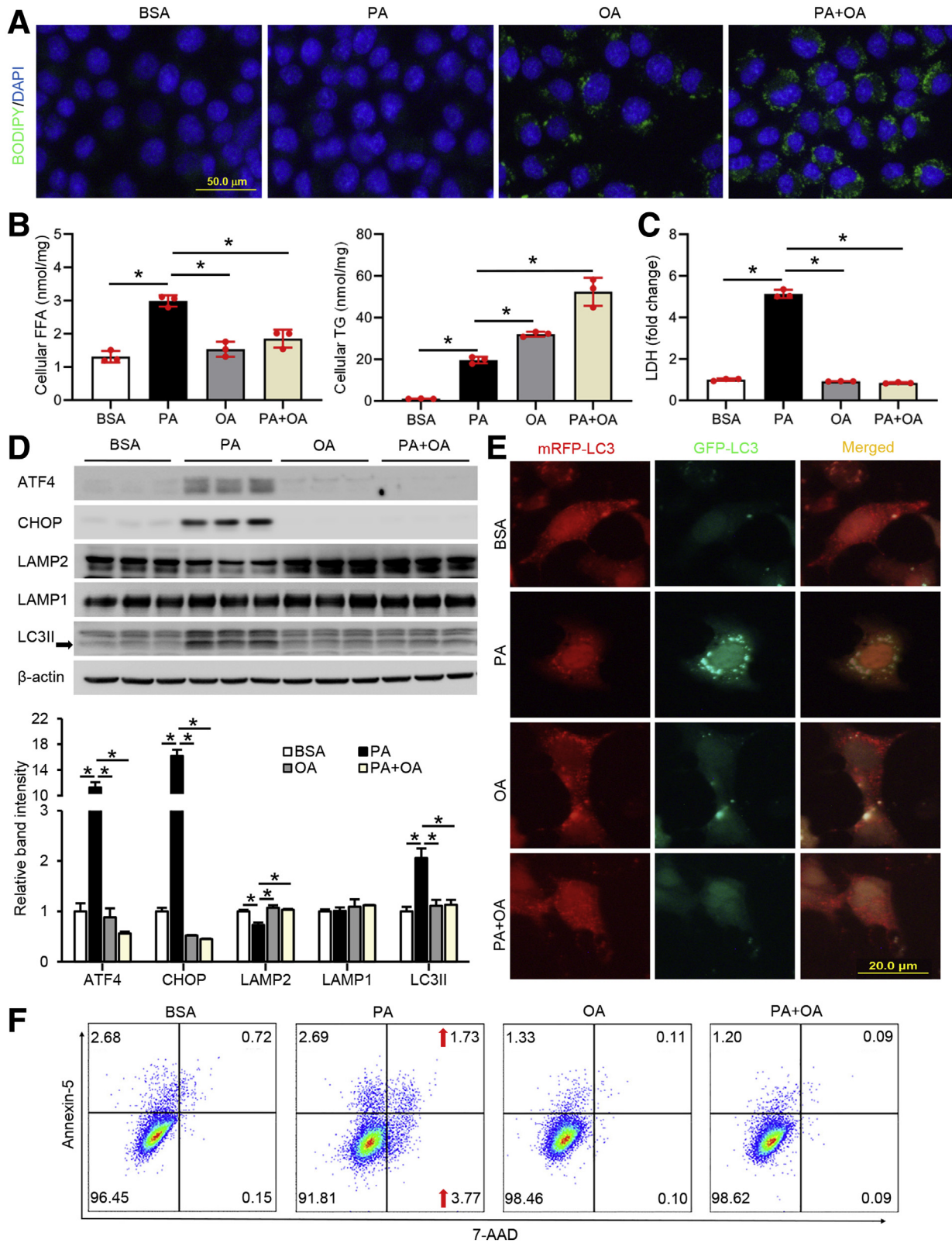


**Figure 4. FFAs but not TG induce ER stress and autophagy dysfunction in hepatocytes.** Hepa-1c1c7 cells, with or without transfection of tandem fluorescent mRFP-GFP-tagged LC3 plasmid (ptfLC3), were treated with 100  $\mu$ mol/L PA, OA, or PA+OA for 24 hours. (A) BODIPY 493/503 staining of cellular neutral lipids accumulation. Scale bars: 50  $\mu$ m. (B and C) Cellular FFA, TG, and LDH measurements. (D) Immunoblot and quantification analysis of cellular protein levels of ATF4, CHOP, LAMP2, LAMP1, and LC3II. (E) Autophagy flux was visualized by immunofluorescence microscopy. Scale bars, 20  $\mu$ m. (F) Flow cytometry analysis of cellular apoptosis. Data are shown as means  $\pm$  SD. \**P* < .05.

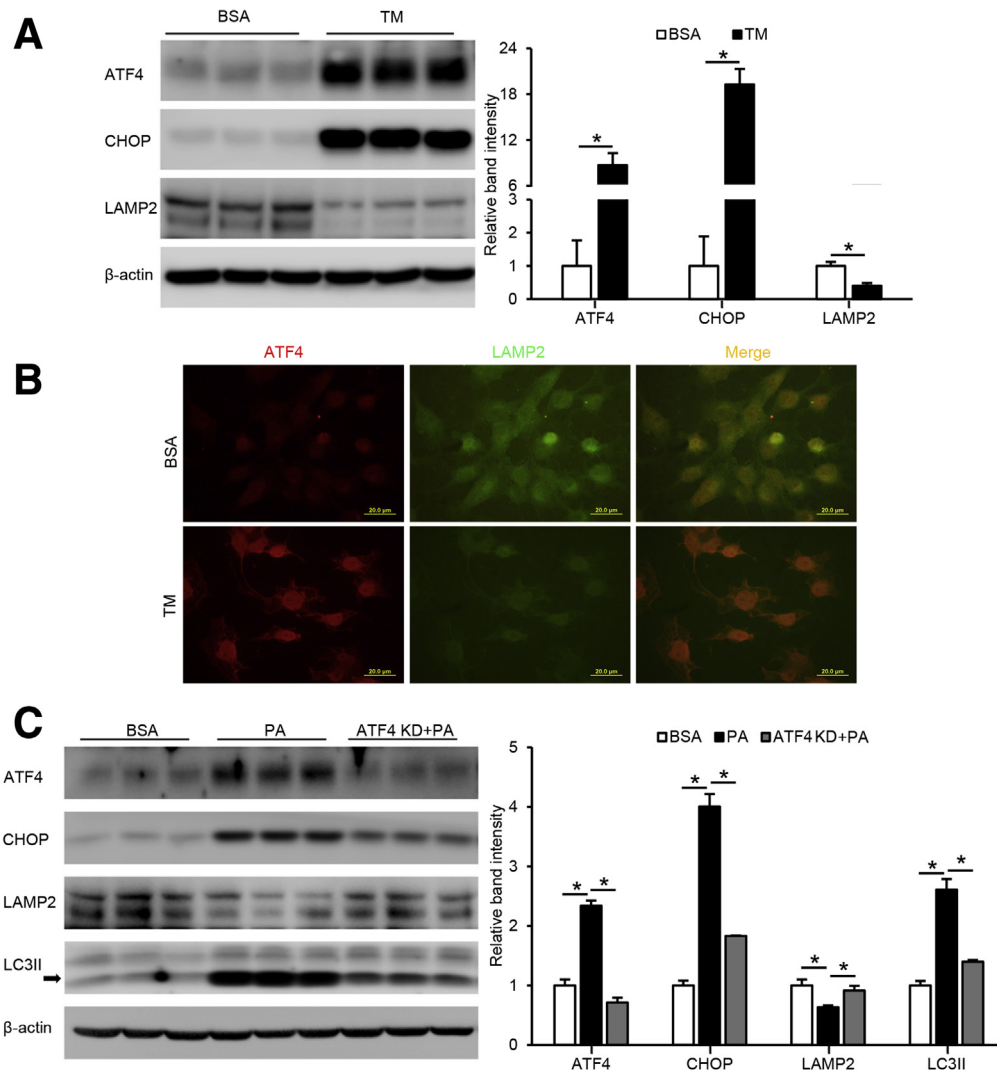


**Figure 5. LAMP2 reduction is a direct downstream event of ER stress in hepatocytes.** (A) Hepa-1c1c7 cells were treated with tunicamycin (TM) at 5  $\mu\text{mol/L}$  for 24 hours and immunoblotted for cellular LAMP2, ATF4, and CHOP. (B) ATF4 and LAMP2 were visualized by immunofluorescence microscopy under tunicamycin treatment. Scale bars, 20  $\mu\text{m}$ . (C) Hepa-1c1c7 cells, with or without transfection of ATF4 knockdown CRISPR plasmid, were treated with 100  $\mu\text{mol/L}$  PA for 24 hours and immunoblotted for cellular ATF4, CHOP, LAMP2, and LC3II. Data are shown as means  $\pm$  SD. \* $P < .05$ .

These data suggest that reducing hepatic fatty acid levels effectively restores LAMP2 and autophagy function via inhibition of ER stress.

### Impaired Autophagy Function in the Liver of Patients With Severe Alcoholic Hepatitis

Our recent study demonstrated that the protein levels of ATF4 and its nuclear distribution were increased in the liver of patients with severe alcoholic hepatitis (SAH).<sup>35</sup> Here, we further determined whether impaired LAMP2-autophagy pathway is associated with ER stress in the pathogenesis of human SAH as observed in the animal study. Western blot analysis showed that the protein levels of LAMP2 were significantly lower, whereas LC3II protein was accumulated in the liver of patients with SAH than that of the control subjects (Figure 9A). In accordance, immunofluorescence analysis demonstrated a reduced cytoplasmic distribution of LAMP2, but an increased abundance of LC3II, in hepatocytes of SAH patients, compared with control subjects (Figure 9B).

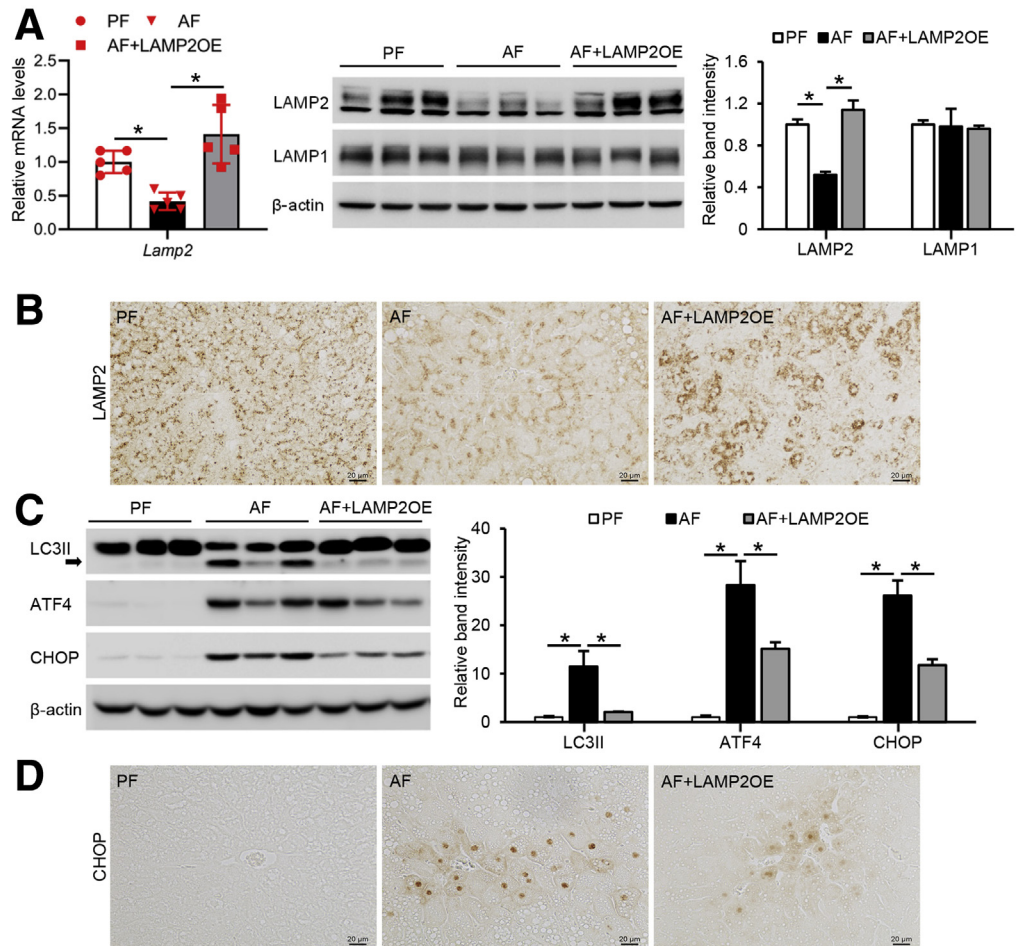
These data suggest that induction of ER stress may account for the disruption of LAMP2-autophagy flux in the development of human SAH.

### Discussion

Excessive hepatic lipid accumulation is frequently observed in ALD patients and animal models. However, it remains unclear whether it is TG or FFAs that incite lipotoxicity and inflammatory responses in the liver. Our results showed that hepatocyte-specific DGAT1 ablation exaggerated alcohol-induced liver injury by increasing hepatic FFAs levels as well as suppressing VLDL lipidation, which leads to elevated liver inflammation, ER stress, and disruption of autophagy. Our cell studies revealed that FFA-mediated induction of ER stress, especially through ATF4, directly targets LAMP2, leading to the suppression of LAMP2 protein and impairment of autophagy flux. We further demonstrated that restoration of autophagy function by overexpressing LAMP2 or pharmacologic induction of



**Figure 6. Hepatocyte-specific LAMP2 over-expression ameliorates organelle dysfunction induced by alcohol in mice.** C57BL/6J mice with or without hepatocyte-specific LAMP2 gene delivery were fed control or alcohol liquid diet for 8 weeks. (A) mRNA expression of hepatic LAMP2 gene, Western blot analysis of LAMP2 and LAMP1 protein (n = 5/group). (B) Immunohistochemistry staining of LAMP2 in liver sections (n = 5/group). Scale bar, 20  $\mu$ m. (C) Immunoblot and quantification analysis of protein levels of LC3II, ATF4, and CHOP (n = 5/group). (D) Immunohistochemistry staining of CHOP on liver tissue sections (n = 5/group). Scale bars, 20  $\mu$ m. Data are shown as means  $\pm$  SD. \**P* < .05. OE, overexpression.



fatty acid clearance by PPAR $\alpha$  agonist Wy14,643 ameliorated alcohol-induced liver injury in mice. Taken together, our study demonstrates that hepatic FFAs are more deleterious in comparison with TG in alcohol-induced lipotoxicity (Figure 9C). Therefore, blocking hepatic TG synthesis alone could be a double-edged sword in battling against the development of ALD if accumulated FFAs are not metabolized efficiently.

Our lab has previously reported that chronic alcohol consumption increases FFA flux from blood to the liver.<sup>6</sup> In accordance, our initial observation confirmed that hepatic DGAT1 is up-regulated by alcohol, which supports the hypothesis that DGAT1 is involved in converting exogenous FFAs into TG. TG-enriched lipid droplets accumulation has long been taken as a gold marker in assessing the progression of ALD. It was believed that suppressing TG synthesis decreases TG-enriched lipid droplets accumulation in the liver, therefore preventing the progression of steatosis.<sup>26,36,37</sup> Nevertheless, suppressing TG synthesis could also lead to the increase of cellular FFAs and other toxic metabolites.<sup>38</sup> Considering that chronic alcohol intake increases FFAs flux from blood to the liver as well as reduces the rate of hepatic FA oxidation, the buildup of FFAs could pose a more deleterious effect to the liver. Indeed, one of the

most important findings of our study is that hepatocyte-specific DGAT1 deletion led to increased levels of hepatocellular FFAs and augmented liver injury in mice fed with alcohol, which strongly supports our hypothesis. We found that once FFAs were incorporated into TG and stored in lipid droplets, less ER stress and cellular injuries were observed, compared with the condition when FFAs were poorly converted into TG. Therefore, hepatic accumulation of TG-enriched lipid droplets may serve as a parallel phenomenon rather than a direct cause of liver injury. Interestingly, what we did not expect was that under the condition of alcohol feeding, DGAT1 deletion increased the amount of TG in mouse liver. It has been reported that DGAT1 participates in VLDL secretion, with one study showing that DGAT1 overexpression in mouse liver increased VLDL secretion<sup>39</sup> and the other showing that DGAT1 is involved in lipidation and maturation of hepatic VLDL particles.<sup>32</sup> Our fast protein liquid chromatography and immunoblot analysis results suggest that DGAT1 may be involved in VLDL lipidation and secretion because DGAT1 deletion resulted in a decrease of serum VLDL-TG levels as well as ApoB100 protein levels after alcohol feeding. Thus, DGAT1-mediated VLDL secretion of TG is an adaptive response to the increased exogenous FFAs influx to

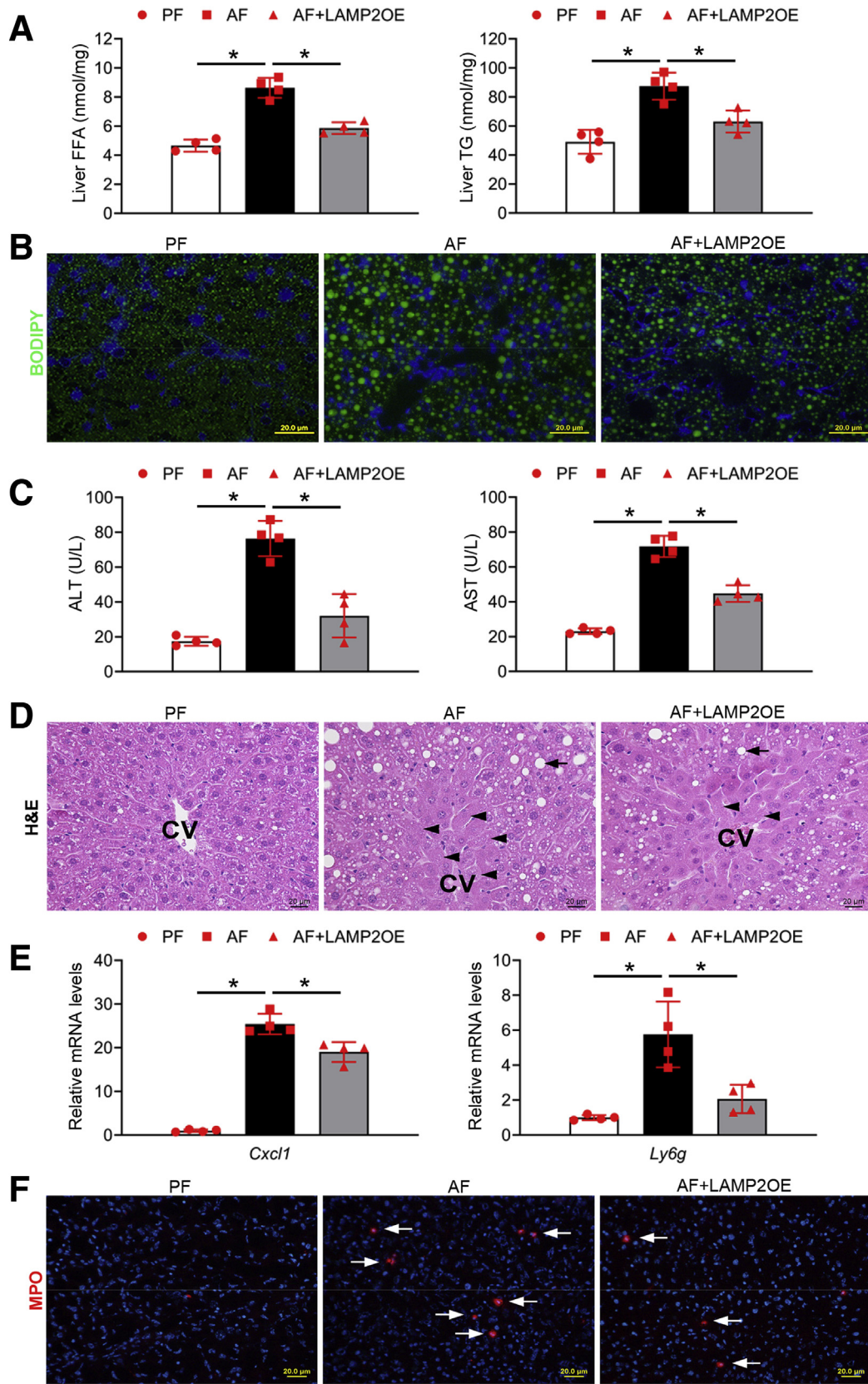


**Figure 7. Hepatocyte-specific LAMP2 overexpression attenuates alcohol-induced lipid accumulation and liver injury in mice.** C57BL/6J mice with or without hepatocyte-specific LAMP2 gene delivery were fed control or alcohol liquid diet for 8 weeks. (A) Analysis of hepatic FFA and TG contents ( $n = 4/\text{group}$ ). (B) BODIPY 493/503 staining of neutral lipids in mouse liver ( $n = 4/\text{group}$ ). Scale bars, 20  $\mu\text{m}$ . (C) Analysis of serum ALT and AST levels ( $n = 4/\text{group}$ ). (D) H&E staining of liver tissue sections ( $n = 4/\text{group}$ ). Arrowheads: hepatocyte degeneration. Arrows: hepatic lipid droplets. Scale bars, 20  $\mu\text{m}$ . (E) *Cxcl1* and *Ly6g* mRNA expression ( $n = 4/\text{group}$ ). (F) Immunofluorescence staining of hepatic MPO positive cells (red) ( $n = 4/\text{group}$ ). Scale bars, 20  $\mu\text{m}$ . Data are shown as means  $\pm$  SD. \* $P < .05$ . CV, central vein; OE, overexpression.

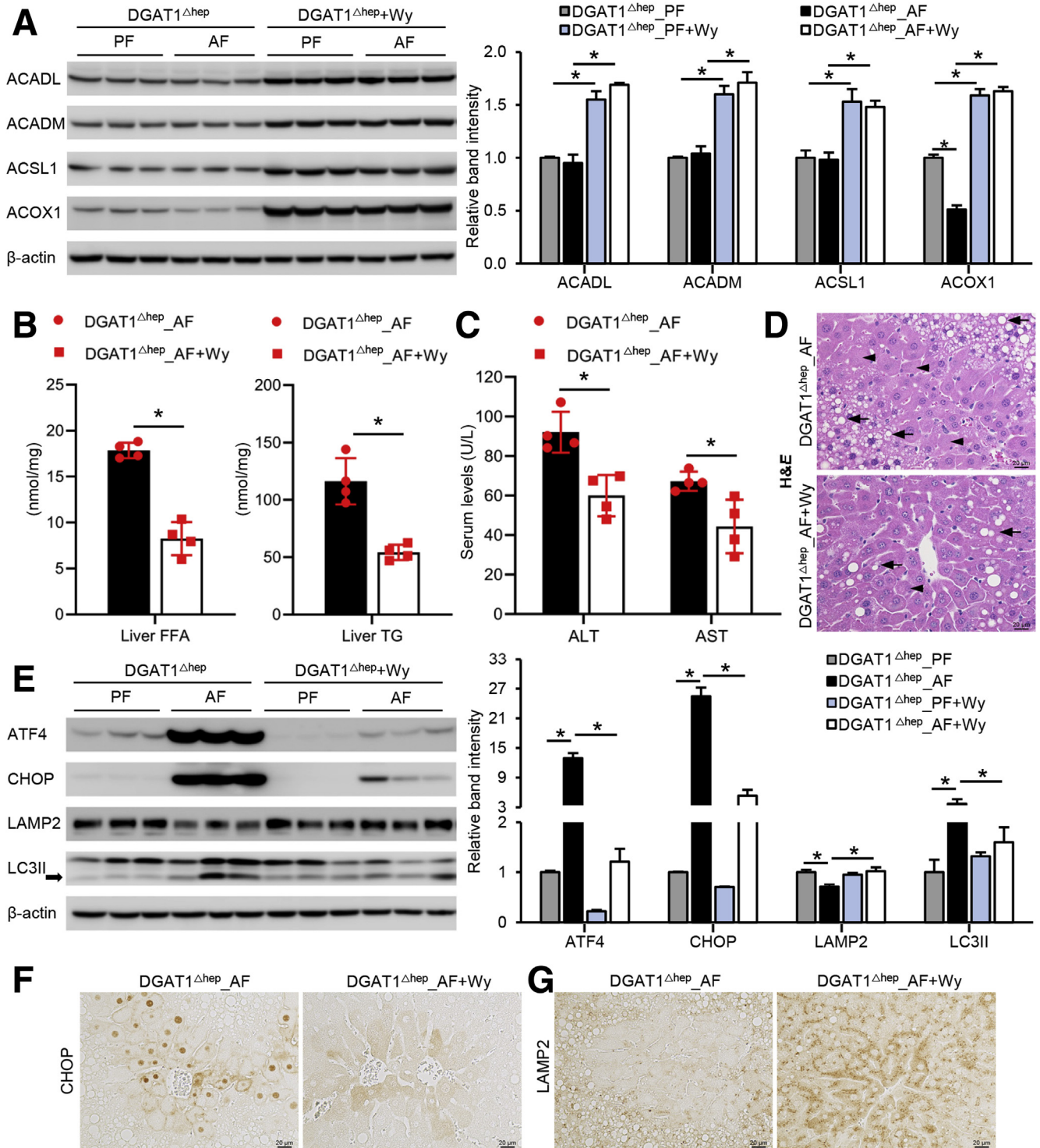


**Figure 8. Pharmacologic activation of PPAR $\alpha$  induces FA metabolism and reverses alcohol-induced liver injury.** DGAT1<sup>Δhep</sup> mice were PF or AF with or without Wy14,643 supplementation at 10 mg/kg/day starting from the last week in 8-week feeding experiment. (A) Immunoblot and quantification analysis of hepatic protein levels of ACADL, ACADM, ACSL1, and ACOX1 (n = 4/group). (B) Analysis of hepatic TG and FFA contents (n = 4/group). (C) Analysis of serum ALT and AST levels (n = 4/group). (D) H&E staining of liver tissue sections (n = 4/group). Arrowheads: hepatocyte degeneration. Arrows: hepatic lipid droplets. Scale bars, 20  $\mu$ m. (E) Immunoblot and quantification analysis of protein levels of ATF4, CHOP, LAMP2, and LC3II (n = 4/group). (F and G) Immunohistochemistry staining of CHOP and LAMP2 on liver tissue sections (n = 4/group). Scale bars, 20  $\mu$ m. Data are shown as means  $\pm$  SD. \*P < .05.

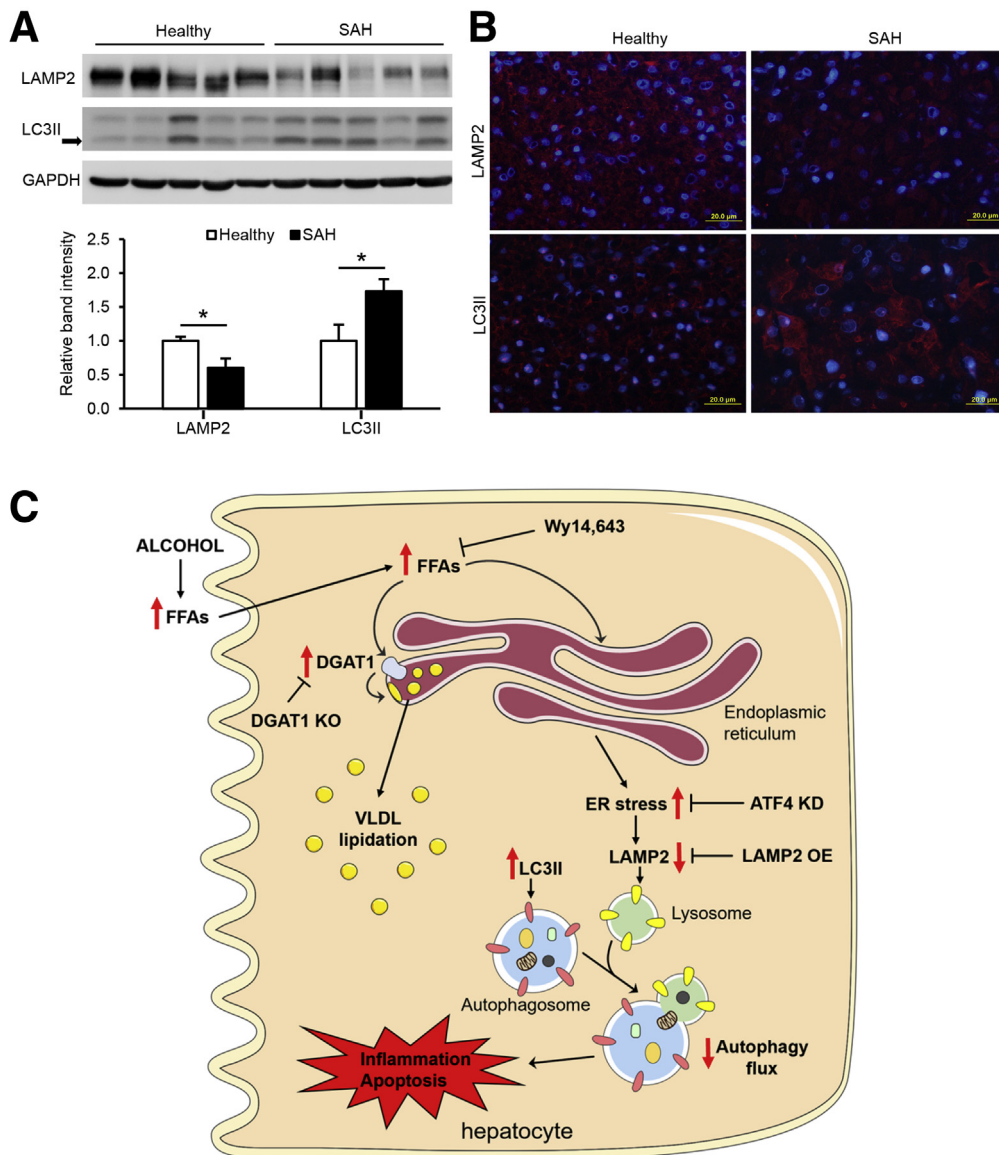


**Figure 9. Impaired autophagy function in the liver of patients with SAH.** (A) Immunoblot and quantification analysis of LAMP2 and LC3II in the liver of healthy subjects and SAH patients (n = 5/group). (B) Immunofluorescence analysis of LAMP2 and LC3II in the liver of healthy subjects and SAH patients (n = 5/group). Scale bars, 20  $\mu$ m. (C) Schematic representation of the role and mechanism of FFA toxicity in the pathogenesis of ALD by inhibiting autophagy flux via inducing ER stress. Data are shown as means  $\pm$  SD. \**P* < .05.

the liver. Because hepatic DGAT2 was also up-regulated by alcohol, further studies are necessary to elucidate how DGAT2 deletion or DGAT1 and 2 double knockout in the liver would affect hepatic lipid homeostasis and the progression of ALD.

Emerging evidence reveals that autophagy is disrupted in animal models of alcohol intoxication. Alcohol exposure has been repeatedly shown to increase hepatic protein level of autophagosome marker LC3II, indicating accumulation of autophagosomes.<sup>31,40,41</sup> However, increased accumulation of autophagosomes may represent either increased synthesis of autophagosomes to meet autophagy demand or suppressed autophagosome-lysosome fusion under cellular toxicity and stress.<sup>42</sup> Growing evidence now supports that LAMP2 is crucial for autophagosome-lysosome fusion during autophagy. Mice deficient in LAMP2 displayed a significant increase of hepatic autophagosomes and LC3II protein

levels.<sup>43,44</sup> Under chronic alcohol exposure, hepatic LAMP2 protein suppression was observed in association with LC3II accumulation.<sup>31,40</sup> In our animal model because DGAT1 deletion resulted in elevated FFAs in the liver under alcohol feeding, we hypothesized that increased hepatic FFAs would further impair autophagy in ALD. Through examining several key autophagic molecules, we identified that hepatic LAMP2 was markedly reduced by DGAT1 deletion, especially under the condition of alcohol exposure, with elevated hepatocellular stress and cell death. Hepatic protein levels of LC3II were induced by alcohol regardless of DGAT1 deletion. Nevertheless, hepatic LAMP1 was not significantly impacted in our in vitro or in vivo studies, suggesting that FFA-mediated toxicity may differentially affect LAMP2 and LAMP1. Importantly, our animal study using LAMP2 transgenic mice demonstrated that restoration of LAMP2 protein normalized hepatic protein levels of LC3II, indicating

improved autophagy activity. Interestingly, LAMP2 overexpression also attenuated alcohol-induced ER stress and liver damage. The present study provides direct evidence supporting a mechanistic link between LAMP2 deficiency and LC3II accumulation in the pathogenesis of ALD. Therefore, our data support that LAMP2 is an important molecular target in ALD.

Molecular mechanisms underlying the regulation of LAMP2 are poorly understood, although the importance of LAMP2 in autophagy flux has been well-documented. Babuta et al<sup>31</sup> demonstrated that micro-RNA 155, which was induced by alcohol, mediated the suppression of both LAMP2 and LAMP1 proteins and resulted in liver damage. A cell study using human trophoblasts observed that induction of ER stress with tunicamycin led to the reduction of LAMP2 and LAMP1 proteins, suggesting that ER stress may negatively regulate LAMP2.<sup>45</sup> ER stress has also been implicated in PA-suppressed selective autophagy. Along with induction of ER stress, PA treatment was found to impair autophagosome-lysosome fusion, although the mechanism remains unclear.<sup>21</sup> These observations led us to speculate that FFA-induced ER stress may negatively regulate the expression of LAMP proteins, which results in the blockade of autophagy flux. Indeed, our *in vitro* studies have confirmed that PA, but not OA, suppressed LAMP2 protein and autophagy flux as PA was poorly converted into TG, therefore inducing more toxicity and cellular injury. We further demonstrated that knockdown of ATF4 restored PA-induced LAMP2 reduction and prevented LC3II accumulation, indicating that ATF4 serves as a negative regulator of LAMP2 and activation of ATF4 contributes to the disruption of autophagy flux under FFA-induced lipotoxicity.

As aforementioned, PPAR $\alpha$  is a well-known master regulator of fatty acid metabolism in the liver.<sup>7</sup> Earlier studies have demonstrated that alcohol exposure leads to PPAR $\alpha$  dysfunction, and reactivation of PPAR $\alpha$  signaling improves fatty acid clearance and alleviates alcohol steatosis.<sup>46</sup> Our animal model demonstrated that hepatocyte-specific DGAT1 knockout further increased FFAs accumulation in the liver and exacerbated alcohol-induced liver injury. Therefore, we sought to determine whether increasing fatty acid clearance through PPAR $\alpha$  activation in DGAT1 $\Delta^{\text{hep}}$  mice would reverse FFA-induced lipotoxicity under chronic alcohol feeding. Our findings support the hypothesis that PPAR $\alpha$  activation by Wy14,643 would reduce the accumulation of hepatic FFAs and subsequent TG synthesis, therefore reversing alcohol-induced hepatocellular damage in DGAT1 $\Delta^{\text{hep}}$  mice. As expected, alcohol-induced hepatic organelle dysfunction has also been markedly improved by Wy14,643 as indicated by neutralized ER stress and restoration of autophagy function. Thus, FFA-induced hepatic lipotoxicity, rather than TG accumulation, may be a possible central mechanism underlying alcohol-induced inflammation and organelle dysfunction in the pathogenesis of ALD.

In summary, the present study demonstrates that alcohol exposure increases hepatic levels of FFAs and TG, and accumulation of FFAs, rather than TG, induces

hepatocellular injury. Mechanistic study showed that FFAs activate ER stress pathway through ATF4, which, in turn, down-regulates LAMP2 and leads to impaired autophagy flux. Overexpression of LAMP2 and reactivation of PPAR $\alpha$  by Wy14,643 in mice both restored autophagy function and ameliorated alcohol-induced liver injury. Down-regulation of LAMP2-autophagy pathway was also detected in the liver of patients with SAH. These findings offer novel insights into the role of hepatic FFAs versus TG in the pathogenesis of ALD and may shed light on the development of therapies targeting FFA-mediated lipotoxicity.

## Materials and Methods

### *Human Liver Samples With SAH*

Liver explant specimens from patients with SAH and wedge biopsies from the donor livers were provided by Johns Hopkins University under the support of NIAAA-funded Clinical Resource for Alcoholic Hepatitis Investigations (R24AA025017) as previously described.<sup>47</sup> Tissue collection of explanted livers or biopsies from donor livers had been approved by Institutional Review Boards at Johns Hopkins Medical Institutions (IRB00107893, IRB00021325).

### *Mice*

C57BL/6J wild-type, DGAT1 floxed mice (DGAT1 $^{\text{floxed/floxed}}$ , stock no. 017322) and albumin-Cre mice (Alb-Cre, stock no. 003574) were purchased from the Jackson Laboratory (Bar Harbor, ME). DGAT1 $^{\text{floxed/floxed}}$  mice were crossed with Alb-Cre mice to generate hepatocyte-specific DGAT1 knockout (DGAT1 $\Delta^{\text{hep}}$ ) mice. For hepatocyte-specific LAMP2 overexpression, 10-week-old C57/BL6J mice were injected with recombinant adeno-associated viral serotype 8 (AAV8) gene transfer vectors (5e<sup>11</sup> GC/per mouse) bearing mouse LAMP2 cDNA (AAV8-LAMP2) controlled by a hepatocyte-specific TBG promoter through retro-orbital sinus as previously described.<sup>35</sup> Mice injected with AAV8-TBG-null vectors served as control (AAV8-Null). Mice were handled and all experiments were performed in accordance with the protocol approved by the North Carolina Research Campus Institutional Animal Care and Use Committee.

### *Chronic Alcohol Feeding and Treatments*

Male mice at 12 weeks old were chronically fed an ethanol-containing Lieber-DeCarli liquid diet (AF) or an isocaloric control liquid diet (PF) as described previously.<sup>47</sup> Sibling littermates of DGAT1 $^{\text{floxed/floxed}}$  mice were used as controls for DGAT1 $\Delta^{\text{hep}}$  mice. All ingredients used in the liquid diets were obtained from Dyets (Bethlehem, PA) except for ethanol (Sigma-Aldrich, St Louis, MO). A PPAR $\alpha$  agonist, pirinixic acid (Wy14,643; Cayman Chemical, Ann Arbor, MI), was supplemented to the diets at 10 mg/kg/day for the last week of the 8-week feeding experiment.

**Table 1.** Primer List

Gene name	Sequence (forward)	Sequence (reverse)
<i>Dgat1</i>	5'-TCCGCCTCTGGGCATTC-3'	5'-GAATCGGCCACAATCCA-3'
<i>Dgat2</i>	5'-CTGGCTGATAGCTGCTCTCTACTTC-3'	5'-TGTGATCTCCTGCCACCTTTC-3'
<i>Cxcl1</i>	5'-CCAGAGCTTGAAGGTGTTGC-3'	5'-AAGCCTCGCGACCATTCTTG-3'
<i>Lamp2</i>	5'-CTGACTCCTGTCTCAGAAAT-3'	5'-GGTGGGAGTTGGTCTTCTT-3'
<i>Ly6g</i>	5'-CCACTCCTCTCTAGGACTTCA-3'	5'-ACCTTGGAACTGCTCTTTC-3'
<i>RPS17</i>	5'-GGAGATCGCCATTATCCCCA-3'	5'-ATCTCCTTGGTGTGCGGGATC-3'

### Western Blot

Whole protein lysates from the mouse liver, serum, and Hepa-1c1c7 cells were extracted using lysis buffer supplemented with protease and phosphatase inhibitors (Sigma-Aldrich). Aliquots containing 30  $\mu$ g of proteins were subjected to sodium dodecyl sulfate-polyacrylamide gel electrophoresis, transblotted onto polyvinylidene difluoride membranes (Bio-Rad, Hercules, CA), blocked with 4% nonfat dry milk in phosphate-buffered saline solution containing 1% Tween-20, and then incubated overnight with the following antibodies, including anti-DGAT1, anti-ApoB100 (Santa Cruz Biotechnology, Dallas, TX), anti-ACSL1, anti-LAMP1, anti-LAMP2, anti-ATF4, anti-CHOP (Cell Signaling Technology, Danvers, MA), anti-ACADL, anti-ACOX1 (Proteintech Group, Inc, Rosemont, IL), anti-ACADM, anti-LC3II (Novus Biologicals, Littleton, CO), anti- $\beta$ -actin, and anti-GAPDH (Abcam, Cambridge, MA), respectively. Membranes were then washed and incubated with horseradish peroxidase-conjugated goat anti-mouse immunoglobulin G or goat anti-rabbit immunoglobulin G (Thermo Fisher Scientific, Rockford, IL). The bound complexes were detected with enhanced chemiluminescence (Thermo Fisher Scientific) and quantified by densitometry analysis.

### Cell Culture and Treatments

Hepa-1c1c7 mouse hepatoma cells (American Type Culture Collection, Rockville, MD) were cultured in Dulbecco modified Eagle medium supplemented with 10% heat-inactivated fetal bovine serum, 100 units/mL penicillin, and 100  $\mu$ g/mL streptomycin (Gibco, Thermo Fisher Scientific, Waltham, MA). Cells were seeded in 6-well plates at a density of  $1 \times 10^5$  cells/cm<sup>2</sup> in 2 mL of standard growth medium per well and reached 80% confluence overnight in 5% CO<sub>2</sub>, 37°C incubator. Then cells were treated with FFAs including PA at 100  $\mu$ mol/L and/or OA at 100  $\mu$ mol/L for 24 hours. FFAs were conjugated to bovine serum albumin at a ratio of 6.6:1, as previously described.<sup>48</sup> Tunicamycin at 5  $\mu$ mol/L was used to treat Hepa-1c1c7 cells for 24 hours.

### Plasmid Transfection for ATF4 Knockdown and Autophagy Flux

Hepa1c1c7 cells were seeded in 6-well tissue culture plates 24 hours before transfection. After cells reached 60%–80% confluency, ATF4 CRISPR/Cas9 KO Plasmid (SC-419228-KO-2; Santa Cruz Biotechnology) and control

CRISPR activation plasmid (SC-437275; Santa Cruz Biotechnology) were transfected to cells following the manufacturer's protocol. Transfection efficiency was determined by Western blot analysis.

To check autophagy flux, Hepa1c1c7 cells were seeded and transfected with pTF-LC3 (plasmid with tandem fluorescent tagged LC3, Plasmid ID # 21074) construct (Addgene, Cambridge, MA). pTF-LC3 construct contains autophagosome marker protein LC3 tagged with both red and green fluorescent protein in tandem (RFP-GFP-LC3). After FFAs treatment, the accumulation of green fluorescent protein and red fluorescent protein signals was visualized using fluorescence microscope.

### Histopathology and Immunohistochemistry

Histopathology staining was performed as previously described.<sup>49</sup> Briefly, liver tissues were fixed in 10% formalin and processed for paraffin embedding. Paraffin sections were cut into 5  $\mu$ m and processed with H&E staining. For immunohistochemistry staining, mouse hepatic LAMP2, CHOP, p-S6, TFEB, and 4-hydroxynonenal (4-HNE) were detected. Paraffin-embedded liver sections were incubated with 3% hydrogen peroxide to inactivate endogenous peroxidases. The endogenous mouse immunoglobulin G was blocked by incubation with a mouse-to-mouse blocking reagent (ScyTek Laboratories, Logan, UT). Tissue sections were incubated with a monoclonal antibody at 4°C overnight, followed by 30-minute incubation with EnVision<sup>+</sup> labeled polymer-horseradish peroxidase-conjugated anti-mouse or anti-rabbit immunoglobulin G (DAKO, Carpinteria, CA).

### Immunofluorescence

To determine hepatic inflammation, cryostat sections of mouse liver were incubated with anti-MPO, followed by Alexa Fluor 594-conjugated donkey anti-rat immunoglobulin G (Jackson ImmunoResearch Laboratories, West Grove, PA). The nuclei were counterstained by 4'-diamidino-2-phenylindole (DAPI; Thermo Fisher Scientific).

### Plasma ALT/AST Levels

Plasma ALT and AST levels were colorimetrically measured by Infinity ALT Reagent and Infinity AST Reagent (Thermo Fisher Scientific), respectively.

### RNA Isolation and Real-Time Polymerase Chain Reaction

Total RNA was isolated from mouse liver tissue and Hepa-1c1c7 cells using TRIzol Reagent (Invitrogen, Waltham, MA) according to the manufacturer's protocol. The complementary DNA (cDNA) was synthesized using the cDNA Synthesis kit (TaqMan Reverse Transcription Reagents; Thermo Fisher Scientific) and amplified with SYBR Green PCR Supermix kit (Qiagen, Hilden, Germany) using a 7500 Real Time PCR System. All primers were designed and synthesized by Integrated DNA Technologies (Coralville, CA). Data were analyzed using the  $2^{-\Delta\Delta C_t}$  threshold cycle method. Primers used for real-time polymerase chain reaction in this study are listed in Table 1. The mRNA levels of genes were normalized to those of RPS17 rRNA and expressed as relative to the control.

### Quantification of TG, FFAs, and VLDL

TG and FFAs from mice liver and hepa1c1c7 cells were measured as previously described.<sup>47</sup> Briefly, lipids were extracted using chloroform/methanol (2:1), vacuumed, and redissolved in 5% Triton X-100/methyl alcohol mixture (1:1 vol/vol). FFA and TG contents were then determined using colorimetric assay kits (Biovision, Milpitas, CA), according to the manufacturer's instructions.

VLDL, low-density lipoprotein, and high-density lipoprotein were isolated from mouse serum.<sup>50</sup> In brief, a Pharmacia Smart System FPLC equipped with a Superose 6 PC 3.2/30 column (GE Healthcare Europe GmbH, Munich, Germany) was used with Dulbecco phosphate-buffered saline containing 1 mmol/L EDTA as a running buffer. After loading 50  $\mu$ L serum, the system was run with a constant flow of 40  $\mu$ L/min, and fractionation was started after 18 minutes with 80  $\mu$ L per fraction. Fraction samples containing serum lipoproteins were used for further analysis to determine TG levels of each fraction. The approximate fraction numbers for VLDL were 17 to 24.

### Cellular Neutral Lipid Staining

Hepa1c1c7 cells were fixed in 4% formaldehyde for 15 minutes at room temperature, permeabilized with 0.2% Triton X-100 in phosphate-buffered saline for 10 minutes, and incubated in 10% normal donkey serum for 30 minutes. Then cells were incubated with boron dipyrromethene (BODIPY) 493/503 dye for 20 minutes and counterstained with DAPI (Life Technologies, Carlsbad, CA) for 1 minute. Accumulation of neutral lipids in the cell was observed by fluorescence microscope.

### Flow Cytometry

The frequency of FFA-treated annexin V (BioLegend, San Diego, CA) and 7-AAD (BioLegend) positive Hepa1c1c7 cells was determined by flow cytometry on FACSMelody (BD Bioscience, San Jose, CA) according to the manufacturer's instructions. The data were analyzed using FlowJo software v10.1 (Treestar, Ashland, OR).

### LDH Assay

LDH assays (Thermo Fisher Scientific) were used to determine cellular LDH activity of Hepa1c1c7 cells treated with FFAs. Briefly, after FFAs treatment, cell culture supernatants were collected, mixed with LDH reaction buffer, and incubated in dark at room temperature for 30 minutes. Then LDH stop solution was added, and LDH release was quantified by measuring absorbance at 490 nm and 680 nm to determine LDH activity.

### Statistical Analysis

All results were analyzed using the independent-samples *t* test or one-way analysis of variance, followed by Bonferroni multiple comparison. Data were expressed as mean  $\pm$  standard deviation (SD). In all tests,  $P < .05$  was considered statistically significant.

### References

1. Sacks JJ, Gonzales KR, Bouchery EE, Tomedi LE, Brewer RD. 2010 National and state costs of excessive alcohol consumption. *Am J Prev Med* 2015;49:e73–e79.
2. Mokdad AH, Marks JS, Stroup DF, Gerberding JL. Actual causes of death in the United States, 2000. *JAMA* 2004; 291:1238–1245.
3. Meikle PJ, Mundra PA, Wong G, Rahman K, Huynh K, Barlow CK, Duly AM, Haber PS, Whitfield JB, Seth D. Circulating lipids are associated with alcoholic liver cirrhosis and represent potential biomarkers for risk assessment. *PLoS One* 2015;10:e0130346.
4. Ohashi K, Pimienta M, Seki E. Alcoholic liver disease: a current molecular and clinical perspective. *Liver Research* 2018;2:161–172.
5. Wei X, Shi X, Zhong W, Zhao Y, Tang Y, Sun W, Yin X, Bogdanov B, Kim S, McClain C, Zhou Z, Zhang X. Chronic alcohol exposure disturbs lipid homeostasis at the adipose tissue-liver axis in mice: analysis of triacylglycerols using high-resolution mass spectrometry in combination with in vivo metabolite deuterium labeling. *PLoS One* 2013;8:e55382.
6. Zhong W, Zhao Y, Tang Y, Wei X, Shi X, Sun W, Sun X, Yin X, Sun X, Kim S, McClain CJ, Zhang X, Zhou Z. Chronic alcohol exposure stimulates adipose tissue lipolysis in mice: role of reverse triglyceride transport in the pathogenesis of alcoholic steatosis. *Am J Pathol* 2012;180:998–1007.
7. Crabb DW, Galli A, Fischer M, You M. Molecular mechanisms of alcoholic fatty liver: role of peroxisome proliferator-activated receptor alpha. *Alcohol* 2004; 34:35–38.
8. Wagner M, Zollner G, Trauner M. Nuclear receptors in liver disease. *Hepatology* 2011;53:1023–1034.
9. Liu J, Han L, Zhu L, Yu Y. Free fatty acids, not triglycerides, are associated with non-alcoholic liver injury progression in high fat diet induced obese rats. *Lipids in Health and Disease* 2016;15:27.
10. Mavrelis PG, Ammon HV, Gleysteen JJ, Komorowski RA, Charaf UK. Hepatic free fatty acids in alcoholic liver

- disease and morbid obesity. *Hepatology* 1983; 3:226–231.
11. Malhi H, Bronk SF, Werneburg NW, Gores GJ. Free fatty acids induce JNK-dependent hepatocyte lipoapoptosis. *J Biol Chem* 2006;281:12093–12101.
  12. Hao L, Sun Q, Zhong W, Zhang W, Sun X, Zhou Z. Mitochondria-targeted ubiquinone (MitoQ) enhances acetaldehyde clearance by reversing alcohol-induced posttranslational modification of aldehyde dehydrogenase 2: a molecular mechanism of protection against alcoholic liver disease. *Redox Biology* 2018;14:626–636.
  13. Mizushima N, Levine B, Cuervo AM, Klionsky DJ. Autophagy fights disease through cellular self-digestion. *Nature* 2008;451:1069–1075.
  14. Yin XM, Ding WX, Gao W. Autophagy in the liver. *Hepatology* 2008;47:1773–1785.
  15. Lin CW, Zhang H, Li M, Xiong X, Chen X, Chen X, Dong XC, Yin XM. Pharmacological promotion of autophagy alleviates steatosis and injury in alcoholic and non-alcoholic fatty liver conditions in mice. *J Hepatol* 2013;58:993–999.
  16. Ding WX, Li M, Chen X, Ni HM, Lin CW, Gao W, Lu B, Stolz DB, Clemens DL, Yin XM. Autophagy reduces acute ethanol-induced hepatotoxicity and steatosis in mice. *Gastroenterology* 2010;139:1740–1752.
  17. Kharbanda KK, McVicker DL, Zetterman RK, Donohue TM Jr. Ethanol consumption reduces the proteolytic capacity and protease activities of hepatic lysosomes. *Biochim Biophys Acta* 1995;1245:421–429.
  18. Baraona E, Leo MA, Borowsky SA, Lieber CS. Alcoholic hepatomegaly: accumulation of protein in the liver. *Science (New York, NY)* 1975;190:794–795.
  19. Mei S, Ni H-M, Manley S, Bockus A, Kassel KM, Luyendyk JP, Copple BL, Ding W-X. Differential roles of unsaturated and saturated fatty acids on autophagy and apoptosis in hepatocytes. *J Pharmacol Exp Ther* 2011; 339:487–498.
  20. Tan SH, Shui G, Zhou J, Li JJE, Bay B-H, Wenk MR, Shen H-M. Induction of autophagy by palmitic acid via protein kinase C-mediated signaling pathway independent of mTOR (mammalian target of rapamycin). *J Biol Chem* 2012;287:14364–14376.
  21. Miyagawa K, Oe S, Honma Y, Izumi H, Baba R, Harada M. Lipid-induced endoplasmic reticulum stress impairs selective autophagy at the step of autophagosome-lysosome fusion in hepatocytes. *Am J Pathol* 2016;186:1861–1873.
  22. Li S, Dou X, Ning H, Song Q, Wei W, Zhang X, Shen C, Li J, Sun C, Song Z. Sirtuin 3 acts as a negative regulator of autophagy dictating hepatocyte susceptibility to lipotoxicity. *Hepatology* 2017;66:936–952.
  23. Yen CL, Stone SJ, Koliwad S, Harris C, Farese RV Jr. Thematic review series: glycerolipids. DGAT enzymes and triacylglycerol biosynthesis. *J Lipid Res* 2008; 49:2283–2301.
  24. McFie PJ, Banman SL, Kary S, Stone SJ. Murine diacylglycerol acyltransferase-2 (DGAT2) can catalyze triacylglycerol synthesis and promote lipid droplet formation independent of its localization to the endoplasmic reticulum. *J Biol Chem* 2011;286:28235–28246.
  25. Wurie HR, Buckett L, Zammit VA. Diacylglycerol acyltransferase 2 acts upstream of diacylglycerol acyltransferase 1 and utilizes nascent diglycerides and de novo synthesized fatty acids in HepG2 cells. *FEBS J* 2012;279:3033–3047.
  26. Villanueva CJ, Monetti M, Shih M, Zhou P, Watkins SM, Bhanot S, Farese RV Jr. Specific role for acyl CoA: Diacylglycerol acyltransferase 1 (Dgat1) in hepatic steatosis due to exogenous fatty acids. *Hepatology* 2009; 50:434–442.
  27. Wei Y, Wang D, Gentile CL, Pagliassotti MJ. Reduced endoplasmic reticulum luminal calcium links saturated fatty acid-mediated endoplasmic reticulum stress and cell death in liver cells. *Mol Cell Biochem* 2009; 331:31–40.
  28. Cazanave SC, Mott JL, Elmi NA, Bronk SF, Werneburg NW, Akazawa Y, Kahraman A, Garrison SP, Zambetti GP, Charlton MR, Gores GJ. JNK1-dependent PUMA expression contributes to hepatocyte lipoapoptosis. *J Biol Chem* 2009;284:26591–26602.
  29. Wang D, Wei Y, Pagliassotti MJ. Saturated fatty acids promote endoplasmic reticulum stress and liver injury in rats with hepatic steatosis. *Endocrinology* 2006; 147:943–951.
  30. Thomes PG, Trambly CS, Fox HS, Tuma DJ, Donohue TM Jr. Acute and chronic ethanol administration differentially modulate hepatic autophagy and transcription factor EB. *Alcohol Clin Exp Res* 2015; 39:2354–2363.
  31. Babuta M, Furi I, Bala S, Bukong TN, Lowe P, Catalano D, Calenda C, Kodys K, Szabo G. Dysregulated autophagy and lysosome function are linked to exosome production by micro-RNA 155 in alcoholic liver disease. *Hepatology* 2019;70:2123–2141.
  32. Irshad Z, Chmel N, Adya R, Zammit VA. Hepatic VLDL secretion: DGAT1 determines particle size but not particle number, which can be supported entirely by DGAT2. *J Lipid Res* 2019;60:111–120.
  33. González-Rodríguez Á, Mayoral R, Agra N, Valdecantos MP, Pardo V, Miquilena-Colina ME, Vargas-Castrillón J, Lo Iacono O, Corazzari M, Fimia GM, Piacentini M, Muntané J, Boscá L, García-Monzón C, Martín-Sanz P, Valverde ÁM. Impaired autophagic flux is associated with increased endoplasmic reticulum stress during the development of NAFLD. *Cell Death Disease* 2014;5:e1179-e.
  34. Pawlak M, Lefebvre P, Staels B. Molecular mechanism of PPAR $\alpha$  action and its impact on lipid metabolism, inflammation and fibrosis in non-alcoholic fatty liver disease. *J Hepatol* 2015;62:720–733.
  35. Hao L, Zhong W, Dong H, Guo W, Sun X, Zhang W, Yue R, Li T, Griffiths A, Ahmadi AR, Sun Z, Song Z, Zhou Z. ATF4 activation promotes hepatic mitochondrial dysfunction by repressing NRF1-TFAM signalling in alcoholic steatohepatitis. *Gut* 2020.
  36. Yu XX, Murray SF, Pandey SK, Booten SL, Bao D, Song XZ, Kelly S, Chen S, McKay R, Monia BP, Bhanot S. Antisense oligonucleotide reduction of DGAT2 expression improves hepatic steatosis and hyperlipidemia in obese mice. *Hepatology* 2005;42:362–371.



37. Monetti M, Levin MC, Watt MJ, Sajan MP, Marmor S, Hubbard BK, Stevens RD, Bain JR, Newgard CB, Sr Farese RV, Hevener AL, Farese RV Jr. Dissociation of hepatic steatosis and insulin resistance in mice overexpressing DGAT in the liver. *Cell Metabolism* 2007; 6:69–78.
38. Yamaguchi K, Yang L, McCall S, Huang J, Yu XX, Pandey SK, Bhanot S, Monia BP, Li YX, Diehl AM. Inhibiting triglyceride synthesis improves hepatic steatosis but exacerbates liver damage and fibrosis in obese mice with nonalcoholic steatohepatitis. *Hepatology* 2007;45:1366–1374.
39. Yamazaki T, Sasaki E, Kakinuma C, Yano T, Miura S, Ezaki O. Increased very low density lipoprotein secretion and gonadal fat mass in mice overexpressing liver DGAT1. *J Biol Chem* 2005;280:21506–21514.
40. Cho H-I, Choi J-W, Lee S-M. Impairment of autophagosome-lysosome fusion contributes to chronic ethanol-induced liver injury. *Alcohol* 2014;48:717–725.
41. Chao X, Wang S, Zhao K, Li Y, Williams JA, Li T, Chavan H, Krishnamurthy P, He XC, Li L, Ballabio A, Ni HM, Ding WX. Impaired TFEB-mediated lysosome biogenesis and autophagy promote chronic ethanol-induced liver injury and steatosis in mice. *Gastroenterology* 2018;155:865–879 e12.
42. Chao X, Ni H-M, Ding W-X. Insufficient autophagy: a novel autophagic flux scenario uncovered by impaired liver TFEB-mediated lysosomal biogenesis from chronic alcohol-drinking mice. *Autophagy* 2018;14:1646–1648.
43. Eskelinen E-L, Illert AL, Tanaka Y, Schwarzmann G, Blanz J, Von Figura K, Saftig P. Role of LAMP-2 in lysosome biogenesis and autophagy. *Mol Biol Cell* 2002; 13:3355–3368.
44. Eskelinen E-L, Schmidt CK, Neu S, Willenborg M, Fuertes G, Salvador N, Tanaka Y, Lüllmann-Rauch R, Hartmann D, Heeren J, von Figura K, Knecht E, Saftig P. Disturbed cholesterol traffic but normal proteolytic function in LAMP-1/LAMP-2 double-deficient fibroblasts. *Mol Biol Cell* 2004;15:3132–3145.
45. Nakashima A, Cheng S-B, Kusabiraki T, Motomura K, Aoki A, Ushijima A, Ono Y, Tsuda S, Shima T, Yoshino O, Sago H, Matsumoto K, Sharma S, Saito S. Endoplasmic reticulum stress disrupts lysosomal homeostasis and induces blockade of autophagic flux in human trophoblasts. *Scientific Reports* 2019;9:11466.
46. Nan Y-M, Wang R-Q, Fu N. Peroxisome proliferator-activated receptor  $\alpha$ , a potential therapeutic target for alcoholic liver disease. *World J Gastroenterol* 2014; 20:8055–8060.
47. Zhong W, Wei X, Hao L, Lin TD, Yue R, Sun X, Guo W, Dong H, Li T, Ahmadi AR, Sun Z, Zhang Q, Zhao J, Zhou Z. Paneth cell dysfunction mediates alcohol-related steatohepatitis through promoting bacterial translocation in mice: role of zinc deficiency. *Hepatology* 2020; 71:1575–1591.
48. Listenberger LL, Ory DS, Schaffer JE. Palmitate-induced apoptosis can occur through a ceramide-independent pathway. *J Biol Chem* 2001; 276:14890–14895.
49. Sun Q, Zhong W, Zhang W, Zhou Z. Defect of mitochondrial respiratory chain is a mechanism of ROS overproduction in a rat model of alcoholic liver disease: role of zinc deficiency. *Am J Physiol Gastrointest Liver Physiol* 2016;310:G205–G214.
50. Wiesner P, Leidl K, Boettcher A, Schmitz G, Liebisch G. Lipid profiling of FPLC-separated lipoprotein fractions by electrospray ionization tandem mass spectrometry. *J Lipid Res* 2009;50:574–585.

---

Received April 30, 2021. Accepted July 1, 2021.

#### Correspondence

Address correspondence to: Zhanxiang Zhou, PhD, Center for Translational Biomedical Research, University of North Carolina at Greensboro, 600 Laureate Way, Suite 2203, Kannapolis, North Carolina 28081. e-mail: z\_zhou@uncg.edu; fax: (704) 250-5809.

#### Acknowledgments

The authors thank Dr Zhaoli Sun at Johns Hopkins University for providing human liver samples.

#### CRediT Authorship Contributions

Wei Guo (Data curation: Lead; Formal analysis: Lead; Investigation: Lead; Methodology: Lead; Validation: Lead; Visualization: Lead; Writing – original draft: Lead)

Wei Zhong (Conceptualization: Supporting; Formal analysis: Supporting; Methodology: Supporting; Software: Supporting; Writing – review & editing: Supporting),

Liuyi Hao (Formal analysis: Supporting; Software: Supporting; Writing – review & editing: Supporting),

Haibo Dong (Software: Supporting; Writing – review & editing: Supporting),

Xinguo Sun (Resources: Supporting),

Ruichao Yue (Writing – review & editing: Supporting),

Tianjiao Li (Writing – review & editing: Supporting),

Zhanxiang Zhou, PhD (Conceptualization: Lead; Methodology: Equal; Supervision: Lead; Writing – review & editing: Supporting)

#### Conflicts of interest

The authors disclose no conflicts.

#### Funding

Supported by the National Institutes of Health grants R01AA018844 and R01AA020212 (Zhanxiang Zhou).